Laser Chem. 1983, Vol. 3, pp. 109–132
0278–6273/83/0306–0110$12.00/0

Printed in Great Britain

Picosecond Processes in Chemical Systems: Vibrational Relaxation§

E. J. HEILWEIL, R. MOORE,‡ G. ROTHENBERGER,†
S. VELSKO and R. M. HOCHSTRASSER

Department of Chemistry, University of Pennsylvania, Philadelphia, PA 19104

A review is presented of our recent studies of vibrational energy relaxation of moderately sized molecules in a variety of media and of the effect of vibrational relaxation on processes such as molecular rearrangements.

Data are presented on intramolecular dynamical processes involving *p*-difluorobenzene and an experiment is described which allows the study of spectral evolution on the picosecond timescale under collision-free conditions.

The vibrational (T_1) relaxation of the apparently simple system consisting of a diatomic CN^- ion in aqueous solution was studied and found to be in the range of a few picoseconds and to be concentration dependent. These results, and the effects of counterions, are suggested to be the result of aggregation of the ions. A discussion of the Raman lineshapes is given in relation to the measured T_1 times.

1. INTRODUCTION

Studies of picosecond processes have now been underway for one and one half decades. The level of detail exposed in experiments has roughly paralleled the advances in laser technology that have taken place during that period. The first applications of picosecond lasers to chemical problems used the solid state lasers neodymium-glass and ruby. The slow repetition rate and poor reproducibility of these systems allowed only rather coarse grain experiments. The attempts to measure statistical limit radiationless processes in azulene[1–3] and benzophenone,[3–5] and studies of nearest neighbor energy transfer

† Supported by the Swiss National Science Foundation.
‡ NSF Pre-Doctoral Fellow.
§ This research was supported by a grant from NSF(CHE 80-00016) and in part by the National Science Foundation, MRL Program, under Grant No. DMR-7923647.

between[6] and within[7] molecules are but few of the processes that were studied with these early picosecond lasers. The important contributions of Kaiser and coworkers on vibrational relaxation in liquids[8,9] involved measurements of coherent Raman scattering and were made possible by more careful control of the Nd:glass laser to generate transform limited TEM_{00} pulses. A subsequent development involved the picosecond generated continuum,[10] which has allowed accurate absorption spectra to be recorded, even at low laser repetition rates, by incorporating extensive multiplexing capabilities.[11]

The current generation of picosecond lasers permits a new level of exploration of molecular processes. The synchronous pumping of dye lasers with cw modelocked gas and solid state lasers provides high repetition rate, high stability picosecond or subpicosecond[12] pulses that were already used in many types of experiments. The stability of these lasers has resulted in them being used effectively in coherence decay experiments on surfaces[13] and in molecular solids.[14,15] The cw-pumped passively modelocked dye lasers pioneered by Ippen and Shank[16] have also found wide applicability in the chemical area by providing opportunities for studies in the 0.2–10 ps regime. More recently the regime less than 0.1 ps was opened up[17] now making it possible for chemists to study directly processes occurring on the timescale of liquid state collisions.

Applications of picosecond laser methods to biological questions have occurred throughout the whole period of development described above. The low repetition solid state devices were used in pump-probe experiments to study the primary processes in vision[18] and photosynthesis.[19] Not unexpectedly, based on the experiences with simpler photophysical processes, the new subpicosecond lasers exposed fast primary events[20–22] not seen in earlier experiments. In addition to photobiological processes, picosecond pulses have been used to perturb biological systems from equilibrium by means of photochemistry, in order that subsequent structural modifications could be followed. One example involves the use of a picosecond pulse to dissociate diatomic molecules O_2, CO or NO from hemoglobin.[23–26] The resulting protein structure change and diatom dynamics in the protein are expected to provide vital clues to the mechanism of hemoglobin cooperativity.

In the present paper a number of experiments are presented which illustrate the state of the art in picosecond (as opposed to sub-

picosecond) methods applied to molecular problems. The theme of the article involves vibrational relaxation.

It is of great interest to generate experimental information on the relaxation dynamics of vibrational states of molecules. In the gas phase, and in the absence of collisions, intramolecular rotational–vibrational energy redistribution cannot onset until the rovibrational levels merge into a quasi-continuum.[27] On the other hand in the presence of collisions the relaxation of a particular level resulting in the redistribution of the energy amongst other translational, rotational and vibrational motions often occurs as rapidly as the hard sphere collision frequency. The situation in a solid is different because of the existence of a quasicontinuum of "external," or lattice modes that can accommodate any amount of the internal vibrational energy. Thus even when excited in the low internal energy region of the vibrational fundamentals the crystal can undergo vibrational energy redistribution. The decay of an internal mode excitation into other internal and external modes is analogous to the relaxation of molecular states excited in the molecular quasicontinuum. We will discuss both these extremes in this article as they occur in preliminary studies of *p*-difluorobenzene vapor[28] and benzene crystals.[14,29–31]

In the solid, just as with the levels of a molecule in regions of high state density, one must distinguish population and phase relaxation processes. The separation of these processes depends on the definition of the "bath" or quasicontinuum states. In the case of the solid there is apparently a clear distinction between lattice and internal mode excitations. Thus we must distinguish experimentally between relaxation involving no alteration in the internal mode, and the relaxation of the internal mode population. In one part of this paper we will deal with a crystalline solid—benzene—so that the excitations are excitons. Each internal vibrational level forms a band of exciton states corresponding to excitation amplitude waves having wavelengths from infinity to the lattice spacing. Since the optical excitation generates only a few of these exciton states for each level, the relaxation of the system into the remaining ones is clearly not a relaxation of the internal mode population. Nevertheless certain experimental techniques measure this relaxation which is analogous to the pure dephasing part of the decay of the coherence of a two-level system.[32,33]

Vibrational energy redistribution and relaxation processes occurring in solutions have quite similar physics to the isolated molecule

and low temperature crystal cases. Rather well-defined molecular vibrational states can be excited in dilute solution and the relaxation occurs both by internal to external mode energy transfer, and by internal energy redistribution. The competition between these two pathways thus determines the nature of the process. In the case of simple diatomic species in liquids the vibrational excitation might couple to local rotations or to external modes. Our recent studies[34] of CN^- in H_2O exemplify this case and are discussed in this article.

An extreme limit of the collision induced relaxation of vibrationally excited molecules occurs in solutions where the collisional frequencies range into the femtosecond regime. Thus a simple barrier crossing process, such as a *cis–trans* isomerization, can be seen as a collisionally induced intramolecular vibrational energy redistribution. In this case the rate is controlled by the effectiveness of collisions in exciting the relevant isomerization mode. Recent results on the photoisomerism of stilbene[35] are described in the last part of this article with emphasis on the relationship of the observed picosecond dynamics to statistical mechanical models.

2. INTRAMOLECULAR VIBRATIONAL RELAXATION IN THE ABSENCE OF COLLISIONS

This section describes the status of our efforts to measure directly the rovibrational energy redistribution in a large molecule. There are many spectral evidences of the nonstationarity of optically accessible rovibrational levels in molecules[36–40] so it seemed necessary to establish the occurrence of these implied relaxations by direct measurements in the time domain. Such measurements are important because there is a regime near to the statistical limit of radiationless transitions where it would not be possible to determine the pathways of vibrational energy redistribution by spectral analysis alone. The study of this "true relaxation region," like that of the statistical limit, will require time resolved spectroscopy to establish the various dynamical pathways.

Our preliminary experiments have involved *p*-difluorobenzene vapor. Even at a few torr, picosecond excitation occurs thousands of times faster than hard sphere collisions so that collision free data can be obtained under bulb conditions if picosecond gating is used. The first experiments to report the time domain identification of

intramolecular vibrational relaxation involved the excitation of levels at 263.2 nm and the subsequent evolution of the fluorescence in the 281.9 nm region.

In the experiment[28] the $3^1 30^3$ level[41] of *p*-difluorobenzene at its 294 K vapor pressure (*c.* 56 torr) was excited by the fourth harmonic (263.2 nm) of a glass laser. The $3^1 30^3$ level is 1616 cm^{-1} above the S_1 zero point level. Gated fluorescence spectra were obtained in the spectral region where the transition $3_2^1 30_3^3$ (281.9 nm) was expected to occur.[42] The energy levels relevant to this experiment are shown in Figure 1.

Spectral evolution of the fluorescence from the $3^1 30^3$ level was expected to occur based on the chemical timing experiments of Parmenter *et al.*[40] and the spectral studies of Kable, Lawrance and Knight.[43] Coveleskie, Dolson and Parmenter[40] studied the effect of added oxygen on the fluorescence spectrum of the $3^1 5^1 30^1$ (2191 cm^{-1}) level of *p*-difluorobenzene vapor and suggested that

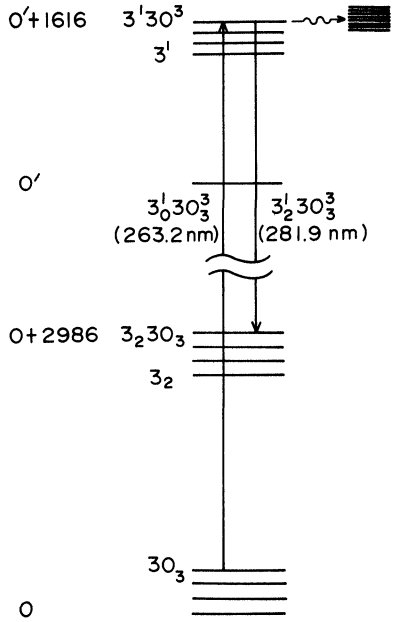

FIGURE 1 Schematic diagram of the main energy levels of *p*-difluorobenzene relevant to the picosecond fluorescence gating experiment.

intramolecular vibrational energy redistribution (IVR) occurs on the 30 picosecond timescale. Kable *et al.*, have obtained evidence that the ν_{30} mode may be a promoting mode for IVR in *p*-difluorobenzene. These experiments suggest that fluorescence originating from a level containing 1600 cm^{-1} excess energy should consist of sharp lines riding on a diffuse background. Furthermore, the intensity ratio of unstructured to structured fluorescence should be *c.* 0.3.

The picosecond gating apparatus is based on a passively modelocked Nd^{3+}: glass oscillator/amplifier system which is shown in Figure 2. The entire pulse train (*c.* 50 pulses of 8 ps duration and 100 μJ average energy) was weakly amplified and a single pulse extracted from the train. This pulse was further amplified to about 5 mJ by a double pass amplifier. The second, third and fourth harmonics of the glass laser were then generated with approximate pulse energies of 1 mJ, 500 μJ and 100 μJ, respectively. The weakly amplified pulse train could be doubled or tripled and the resulting harmonics used to synchronously pump two cavity dumped dye lasers.

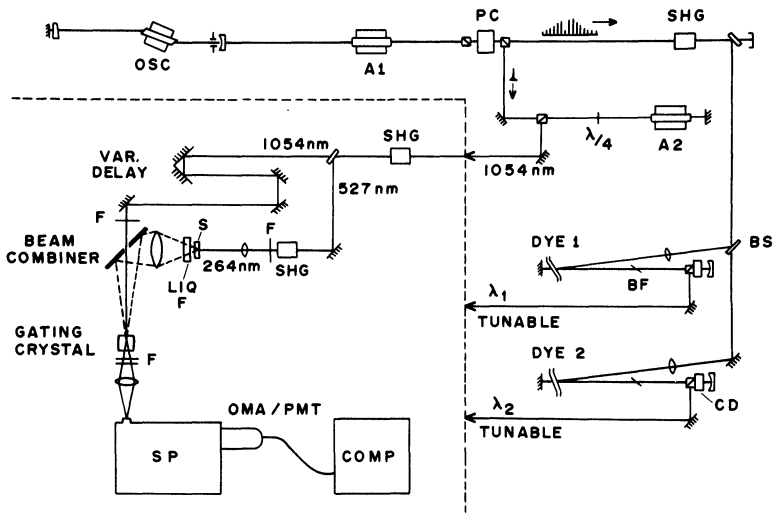

FIGURE 2 High repetition rate glass laser-dye laser system. The picosecond fluorescence gating apparatus is enclosed in the dotted box. The laser is designed for rapid change over between experiments which involve different pulse sequences and laser frequencies. The various components are: OSC (oscillator); A (amplifier); PC (Pockels cell); SHG (frequency doublers); BS (beam splitter); BF (birefringent filter); CD (cavity dumper); SP (spectrograph); F (filter); LIQ. F. (liquid chemical filter); S (sample).

The dye lasers were tuned by birefringent filters to produce 20 μJ pulses of about 2 ps duration.

In the gating experiment fluorescence from the sample was filtered to remove luminescence at the UV detection wavelength, collected by a lens, and directed into a KDP crystal where it was combined with the fundamental of the laser. The KDP crystal was oriented such that the difference of the fluorescence and laser pulse frequencies is generated. The down converted fluorescence was imaged on the slit of a spectrometer and detected with an optical multi-channel analyzer or a phototube. By delaying the arrival of the laser pulse, a time scan of the fluorescence spectrum could be obtained. The gate width was measured to be 10 ps.

The downconverted fluorescence spectrum was obtained at a time delay of ~6 ps. Two of the peaks, corresponding to the expected positions of the $3_2^1 30_3^3$ (281.9 nm) and $3_1^1 5_1^0 6_1^0 30_3^3$ (282.2 nm) transitions, are shown in Figure 3. The regions immediately on either side of these two peaks are "unstructured." The intensity ratio of the unstructured to structured ($3_2^1 30_3^3$) portions of the spectrum was found to be 0.5. The downconverted spectrum is a single vibronic level fluorescence.

Kinetic studies were carried out to ascertain the time dependence of the spectrum. The results are shown in Figure 4. These data show that the emission from the unstructured region (Figure 4b) is delayed in its appearance relative to the emission from the peak region (Figure 4a). These preliminary data fit to a model in which the initially pumped $3^1 30^3$ level decays into nearby rovibronic levels. Our early data do not allow for a precise determination of this intramolecular vibrational relaxation rate, but we are able to say that it is on the order of 6 ps, and is certainly less than 10 ps.

3. VIBRATIONAL ENERGY RELAXATION OF IONS IN SOLUTION

An important aspect of chemical physics that is currently attracting much attention is the determination of the mechanisms responsible for vibrational relaxation in the ground electronic states of molecules.[44–47,9] Information of this type would help to clarify the way in which energy redistribution contributes to thermally assisted reaction rates. Of primary interest is to uncover vibrational relaxation

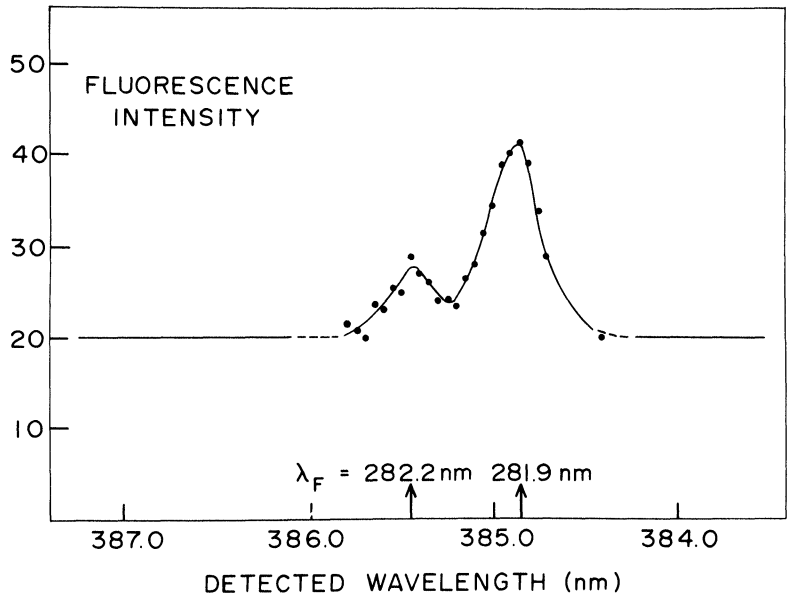

FIGURE 3 Portion of the fluorescence spectrum of *p*-difluorobenzene gated at 6 ps (294 K, equilibrium vapor pressure; *c.* 56 torr). The arrows indicate the expected positions of the $3_1^1 5_1^0 6_1^0 30_3^3$ (282.2 nm) and $3_2^1 30_3^3$ (281.9 nm) transitions. The solid lines on either side of the peaks represent the average of many data points. Within the error of our measurements, no structured emission was observed in these regions.

pathways and rates in solution, where many chemical reactions take place. To this end, most attention has been paid to room temperature neat liquids and a few solutions of organic compounds.[9] Since these systems exhibit picosecond relaxation times, elaborate techniques involving pulsed tunable IR pumping and picosecond anti-Stokes–Raman probing have generally been employed.[9,48,40]

We have undertaken a course of study to further explore vibrational energy relaxation of ionic solute molecules in aqueous solution at room temperature. This class of systems has been chosen because ionic compounds include the simple diatomic ions, so that we expect to bring our results into relationship with theory. In addition, the solubility of many inorganic salts can be extremely high (up to 10 moles/liter) in water, which makes feasible measurements by current pulsed laser techniques.

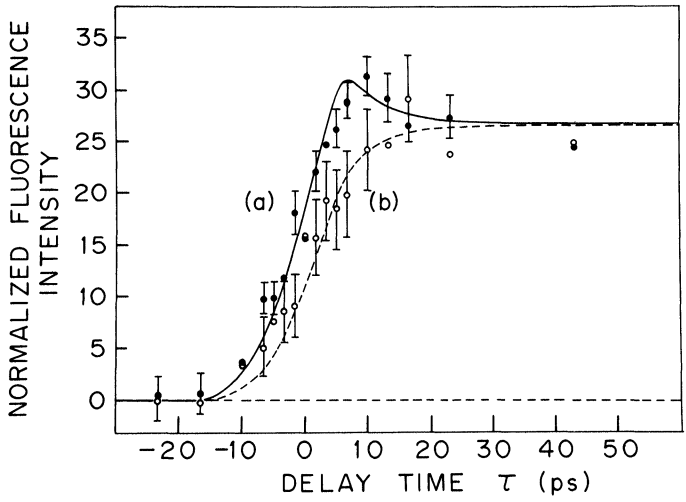

FIGURE 4 Time evolution of the structured (a) and unstructured (b) fluorescence of *p*-difluorobenzene. The solid lines are drawn from a model in which the structured emission decays into nearby rovibronic levels. The long time (40 ps) intensity ratio of structured to unstructured fluorescence is 2:1. The data are normalized to this long time value to facilitate comparison of the growth kinetics.

T_1 relaxation of aqueous CN^- ion Our preliminary results of the diatomic anion CN^- in H_2O/D_2O (Na^+ and K^+ salts) are reviewed here.[34] Of particular interest to us was the concentration dependence of the vibrational energy relaxation rate ($1/T_1$) and how T_1 measurements related to the CN-stretch Raman linewidths of these same solutions. The elucidation of relationships between the observed relaxation times and Raman spectra were expected to lead to a clearer picture of energy relaxation contributions in more complex systems such as the SCN^- ion and higher cyanide containing homologs, and perhaps larger molecular ionic species.

The method employed in this study is an extension of that used by Laubereau and Kaiser.[9] The laser system used for our picosecond experiments has been described in Section 2 above. Briefly, an amplified single pulse from this laser (4 mJ) was used to produce second (527 nm, 0.5 mJ) and third (351 nm, 150 μJ) harmonic pulses (about 8 ps duration). A third pulse from the synchronously pumped Rhodamine-B dye laser (592 nm, 10 μJ) was then combined with the 527 nm pulse and focused colinearly by an achromatic lens into a

5 cm cell containing a saturated solution of NaCN. This cell sufficiently amplifies the dye laser pulse by the SRS process so that the resulting two fields can be used to pump the CN-stretching vibration ($2080\ cm^{-1}$) in a second cell (0.5 to 10 mole/liter solutions). After exciting about 3% of the solute species by this stimulated Raman gain process, the intantaneous population in $v = 1$ is probed by the anti-Stokes scattering of the variable-delayed 351 nm pulse. Collection of this anti-Stokes signal (I_{AS}) by standard Raman optics as a function of delay maps out the population relaxation time, T_1.

The time-dependence of the I_{AS} signal for a saturated solution (relative concentration of unity) of NaCN in H_2O or D_2O exhibited a pulse-width limited decay of not greater than 5.0 ps. In more dilute solution ($[CN^-]_{rel} = 0.2$ or 2.0 molar), we observed a lengthening of the T_1 time to about 7.0 ± 1.0 ps. By monitoring the I_{AS} peak intensity at $t = 5$ ps as a function of concentration, one can then obtain the $1/T_1$ relaxation rates corrected for excitation and concentration effects and normalized to the $[CN^-]_{rel} = 0.2$ absolute decay measurement. The log of these $1/T_1$ rates with their respective error limits are shown as the triangles in Figure 5 as a function of $[CN^-]_{rel}$.

According to this analysis, it is clear that the T_1 relaxation is concentration dependent. Down to *c.* 0.5 of saturation, the value of $1/T_1$ changes only slightly going through a maximum near 0.8 (about six H_2O/CN^- mole ratio). At 0.5 of saturation, T_1 is observed to undergo a sudden decrease.

Relation of T_1 relaxation to Raman lineshapes Under particular circumstances, it should be possible to extract relaxation information from frequency domain measurements of vibrational modes. Theoretical efforts have been placed on determining contributions from dephasing and energy relaxation mechanisms to spectral lineshapes.[50,51] Overall, the total vibrational dephasing rate, $1/T_2$ (related to the Raman full linewidth at half-maximum $\Delta\nu\ cm^{-1}$ for a Lorenzian band by $1/T_2 = \pi\Delta\nu c$) is composed of a "pure" dephasing rate, $1/T_2^*$ produced by translational collisional perturbations plus rates due to energy relaxation, $1/T_1$, resonance energy transfer, inhomogeneous broadening, etc. It has been found from a variety of measurements of T_2 in cryogenic liquids[45] and room temperature liquids[9] that the T_1 contribution cannot, *a priori*, be extracted from the Raman lineshape and that the pure dephasing process dominates the width.

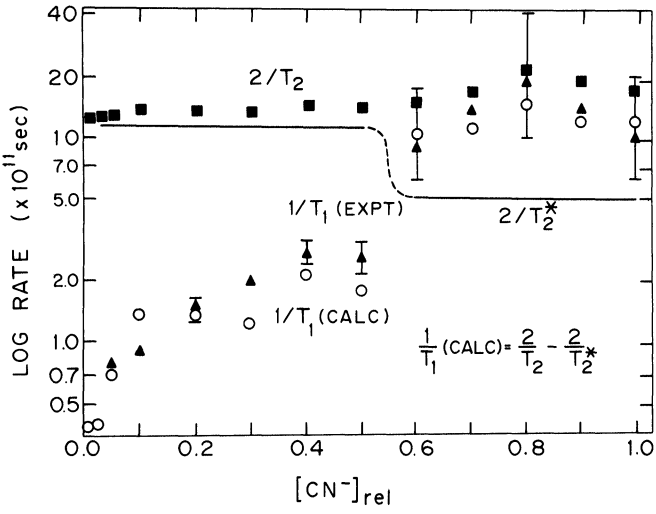

FIGURE 5 Calculated $1/T_1$ vibrational relaxation rate (○) derived from Eq. (1) using the experimentally determined dephasing rate $1/T_2$ from isotropic Raman linewidths (■) and a "pure" dephasing rate $1/T_2^*$, indicated by the solid line. The log of these rates and the measured vibrational relaxation rate $1/T_1$ (▲) obtained at 25°C are shown as a function of CN^- concentration. $[CN^-]_{rel} = 1.0$ is for a saturated 9.6 mol/liter NaCN solution.

Recent measurements of Raman spectra in aqueous NO_3^- [52] and HgI_4^{-2} [53] solutions have addressed this problem and indicate that temperature variations in HgI_4^{-2} solutions of the 123 cm^{-1} ν_1 band are due to changes in T_2^*. The concentration effects observed for the $\nu_1(A_1')$ NO_3^- band in H_2O from 6 to 13 cm^{-1} are attributed to T_2^* inhomogeneous broadening with the Kubo model[50] modulation time ($\tau_c = 0.3$ ps is related to collision times) being nearly constant. In both of these analyses, $1/T_1$ rates were assumed to be negligible. Armed with our measured T_1 times for CN^-, it should be possible to determine the extent that T_1 actually contributes to the Raman linewidth.

A careful analysis of the spontaneous Raman lineshapes for the CN^- solutions shows that there are two highly polarized Lorenzian components which change in magnitude as a function of concentration. The height of the smaller, higher energy peak is most significant at 0.5 concentration. This band is presumably due to ionic aggregation or some type of $Na^+—H_2O—CN^-$ ion pairing which is also observed

in other Na^+ salts.[54] All solutions of KCN in H_2O, however, have one Lorenzian peak in the CN-stretch region, and the NaCN/KCN linewidths are the same for very dilute solutions. Deconvolution of the NaCN bands to obtain the linewidth of the much larger "free cyanide" component (populated by Raman gain) shows a distinct correlation between the T_1 dependence obtained by our time-domain measurements and the linewidth.

Neglecting contributions to the total T_2 dephasing time from resonant V–V transfer, we assume a rate relationship of the form:

$$\frac{2}{T_2} = \frac{1}{T_1} + \frac{2}{T_2^*} \tag{1}$$

As was found in the nitrate study,[52] we also assume that pure dephasing dominates the linewidth. Then, using the observed Raman linewidths ($1/T_2$) corrected for slit width and depicted as squares in Figure 5, one can subtract a chosen $1/T_2^*$ rate (the solid line in the figure) to obtain the "best fit" $1/T_1$ (calc) values shown as the circles. These results also suggest that the rate increase at $[CN^-]_{rel} = 0.5$ is indeed a real effect, and that for concentrations ≤ 0.05 molar, the dilute T_1 limit is about 25 ps. It should be noted that the "dilute" T_2^* determined here is 0.4 ps. This time constant might be related to the rotational correlation time or jump model rest time which was determined to be 0.8–0.9 ps in 4 molar KCN solutions by means of IR and Raman isotropic and anisotropic profiles.[55] The vibrational dephasing mechanism in this case could be mainly determined by the quasi-free rotation time of the CN^- ion.

It appears that for increasingly concentrated solutions at room temperature, the observed CN^- Raman line broadening from the dilute full width of 6.8–10.5 cm^{-1} at saturation is mostly due to an increase in the vibrational population relaxation rate. Further studies are in progress to determine more accurately the dilute T_1 limit, and whether this relaxation is sensitive to local environment (cation type, water structure) or the addition of alternate intramolecular pathways (in SCN^-). It is anticipated that a more complete picture of water[56] and concentrated electrolyte solutions may then lead to a better understanding of vibrational energy relaxation and redistribution in solutions.

4. VIBRATIONAL RELAXATION AND TRAPPING IN MOLECULAR CRYSTALS

The conceptual basis for understanding vibrational dynamics in crystals is the same as that for isolated molecules. A low temperature crystal is an approximate realization of the limit of an infinitely large molecule in a well defined initial state. Since the interactions and densities of crystal states are often known from spectroscopic measurements, crystals represent a useful model for understanding the general principles which govern vibrational relaxation in large systems. In addition, the concepts which arise in crystal relaxation are an important bridge between the pure quantum mechanical description of vibrational relaxation in isolated molecules and the statistical description of relaxation in condensed media at finite temperatures.

Vibrational coherence decay in molecular crystals arises from both quasi-elastic, or dephasing, processes and from population relaxation. Dephasing due to phonon scattering has a pronounced temperature dependence, decreasing as the temperature decreases and vanishing at the absolute zero. In addition, in any real crystal, there are strains and impurities which cause scattering and hence dephasing. Population relaxation can occur through decay to lower vibrational levels of the host material ("self trapping") or through energy transfer to impurities. In order to account properly for all of these processes, it is necessary to know the band structure of the vibration of interest, and for the reason we have chosen to study the 991 cm^{-1} mode of benzene.

The width[14] of the 991 cm^{-1} band is about 1.05 cm^{-1}, with the four $\mathbf{k} = 0$ Davydov components in the relative order A_{1g} (0 cm^{-1}), B_{3g} (0.47 cm^{-1}), B_{2g} (0.53 cm^{-1}) and B_{1g} (1.05 cm^{-1}). By choosing the laser polarizations parallel to the **b** crystallographic axis, the A_{1g} components may be preferentially excited. The fact that the Raman driven level lies at the band bottom where the density of states is vanishing, provides a great simplification to the interpretation of the observed coherence loss in this state. In addition, only six internal vibrational states lie below 991 cm^{-1} and of these only two, ν_{12} at 976 cm^{-1} and ν_{10} at 855 cm^{-1} lie within the spectrum of one phonon lattice excitation.

We have measured the coherence loss of the benzene 991 cm^{-1} mode (A_{1g} component) by the time resolved CARS technique. In this experiment, two synchronously pumped dye lasers are tuned so that their difference frequency is 991 cm^{-1}. The higher frequency laser is split into two beams of equal intensity. The pulses in one of these beams are made time coincident with the pulses from the second, lower frequency laser to form a "pump pair" which excites the sample by stimulated Raman scattering. The pulses in the other part of the high frequency laser beam can be time delayed with respect to the pump pair. These pulses probe the coherent amplitude remaining at a time delay τ after the pump pair has excited the crystal by stimulating coherent anti-Stokes emission. The intensity of this emission as a function of time delay is the time resolved CARS signal. For noise burst pulses,[57] this signal can be written:[29]

$$I_3(\tau) = \int_{-\infty}^{\infty} R^2(t')Q(\tau - t')\,dt' + BQ(\tau) \tag{2}$$

where $R(t)$ is the Raman response function, i.e., the Fourier transform of the Raman lineshape. The "instrument function" $Q(t)$ is the third order correlation function of the pump and probe pulses and is obtained from the CARS signal in liquid benzene, where the dephasing time is only a few picoseconds. The convolution structure obtains in our experiment because of the noise burst properties of dye laser pulses. Since the coherence time of the noise in our pulses is much less than the time duration of each pulse (2 ps, vs. 8 ps) interference among amplitudes at different times during the excitation pulse are averaged out and the signal is approximately the sum of *intensities* even for coherence times of the order of the pulse duration. The second term in $I_3(\tau)$ is a coherence artifact arising because the high frequency pump and probe pulses are derived from the same dye laser and hence have correlated noise substructure. The use of Eq. (2) allows us to extract dephasing times which are of the order of the pulse duration (~10 ps).

Figure 6 shows the excellent fit to our data obtained using Eq. (2). In this case, the data is for a pure benzene crystal at 1.6 K. $R(t)$ is taken to be a single exponential with a time constant of 80 ps. We have argued previously[14,29–31] that this decay represents a population relaxation process. Recently, Califano and co-workers[58] calculated the rate of population decay from this state in the benzene crystal

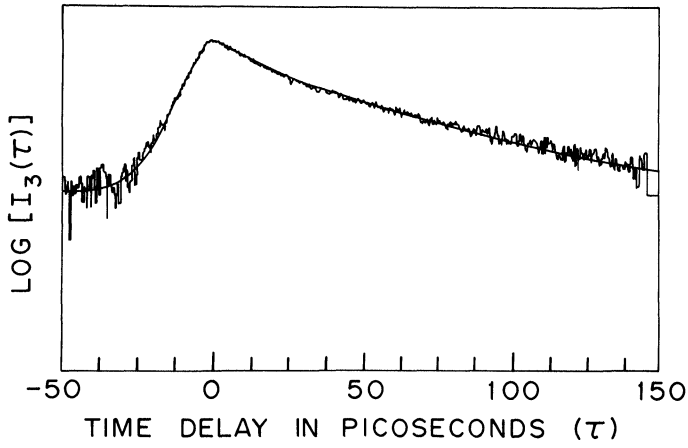

FIGURE 6 Log of coherent antistokes signal intensity versus delay time for pure benzene A_g (991 cm^{-1}) at 1.6 K. Solid line is a least squares fit using Eq. (2) and an exponentially decaying response function.

and found a relaxation time of 50 ps. The primary channel into which population relaxes is ν_{10}.

We have also studied mixed proto/perdeutero benzene crystals. The addition of 10% perdeutero benzene to the proto host causes a two fold increase in the coherence decay rate. To understand the concentration dependence of the coherence decay it is necessary to consider the effects of impurities in the separated band limit, i.e. when the impurity states lie well outside the width of the relevant host vibrational band. In this case frequency matching between host and impurity is poor, so that excitation by the relatively narrow pump pulses doesn't penetrate the impurity centers. Hence the initial state created in our experiment can be written as:

$$|\psi(0)\rangle = \sum_j \zeta_j |j\rangle \tag{3}$$

where ζ_j is a random variable equal to 1 if site j is occupied by a host molecule and 0 if by an impurity. The set $\{|j\rangle\}$ is the site basis for the host material. In terms of this initial state, the Raman response function is

$$R(t) = \langle\langle \psi(0)|\psi(t)\rangle\rangle_{\text{conf}} \tag{4}$$

The outer brackets in this expression represent a configurational average over impurity sites. In general, $R(t)$ decays because of both impurity scattering and energy trapping. However, it is possible to show[29] that for small impurity concentrations, the coherence decay law is:

$$R(t) \propto e^{-(t/\tau)^{1/2}} \tag{5}$$

for a state like 991 cm^{-1} A_{1g}, which is located near a band point where the density of states is asymptotically vanishing. For the A_{1g} component in particular, detailed calculation shows that

$$\tau = C_B^{-2} A \tag{6}$$

with $A = 2 \times 10^{-11}$ s and C expressed as mole fraction. Thus, both the form of the decay law and the characteristic timescale for dephasing make it seem unlikely that impurity scattering is significant in this system, even at impurity concentrations of 15% or more.

The nature of initial state (3) has important consequences for the concentration dependence of energy trapping. The total energy decay rate in a mixed crystal in the separated band limit[29] has the following form:

$$k = k^{(0)} + C_A^2 n^2 k_{AA} + C_A C_B n k_{AA} + C_A C_B n^2 k_{AB} + C_B^2 n k_{AB} \tag{7}$$

Here C_A and C_B are the mole fractions of host and impurity molecules. k_{AA} and k_{AB} are overall site–site energy transfer rate constants for host–host and host–guest energy transfer, and n is an effective number of nearest neighbors surrounding an excited host site. $k^{(0)}$ represents the single site self-trapping rate constant, and hence is concentration independent. The total rate in Eq. (7) is the sum of coherent ($\sim n^2$) and incoherent ($\sim n$) energy transfer processes. In the limit of the pure crystal, $C_A = 1$ we have

$$k_0 = k^{(0)} + n^2 k_{AA}, \tag{7a}$$

while in the infinite dilution limit $C_B = 1$ we have

$$k_\infty = k^{(0)} + n k_{AB}. \tag{7b}$$

A striking conclusion of this description is that even if the trapping efficiency of the impurity is equal to the self trapping efficiency $k_{AB} \approx k_{AA}$) the rate of energy decay will *decrease* with addition of impurity molecules simply because the coherence of the energy transfer process is being lost.

Figure 7 shows the "global" concentration dependence of the vibrational energy trapping rate in C_6H_6/C_6D_6 mixed crystals. Included on this graph is a point at 2% proto in perdeutero host.[30] Since the infinite dilution rate constant k_∞ approximately equals the pure crystal rate k_0, Eqs. (7) imply that $nk_{AB} \approx n^2 k_{AA}$ for the 991 cm^{-1} A_{1g} state. This conclusion is consistent with the fact that the number of single quantum decay channels available in C_6D_6 is nearly three times the number in C_6H_6.

5. ISOMERIZATION OF MOLECULES IN SOLUTIONS

Chemical reaction dynamics in the liquid phase has been an area of renewed theoretical interest in the past few years.[59] The effect exerted by the solvent on the rate of a chemical reaction has been described by frictional[60–64] and collisional[65–68] models. From the point of view of the experimentalist, the validity of these models can however be checked only with systems for which the different reactive processes studied are sufficiently well defined. Conformational or *cis–trans*

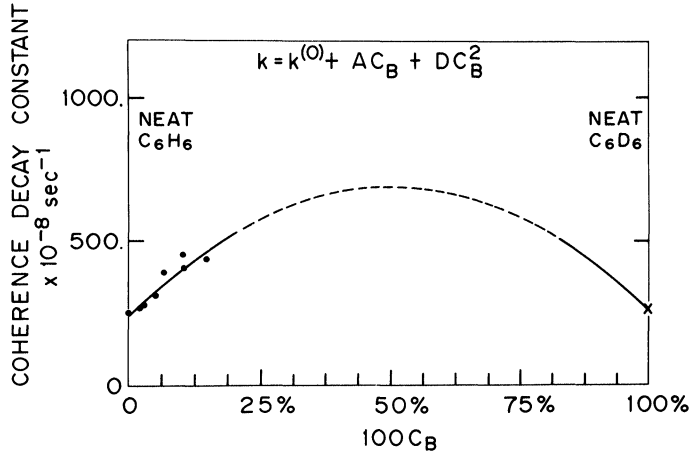

FIGURE 7 Coherence decay rate of the 991 cm^{-1} mode in mixed proto/perdeutero benzene crystals at 1.6 K as a function of perdeutero concentration (C_B). The line is a fit using Eq. (7) and the identity $C_A + C_B = 1$. The dashed portion indicates the "percolation" regime where scattering effects may be important. X is the dilute proto in deutero host measurement from Ref. 30.

isomerizations seem to be good candidates for the purpose of testing theoretical models: they are unimolecular and therefore the problems of reactant diffusion or reactive collision frequency are avoided; in favorable cases, the isomerization process can be described by one reaction coordinate only. A number of comparisons of experimental data on isomerization kinetics with theoretical models are reported in the literature. For example, Garrity and Skinner[69] report on a qualitative agreement of an NMR study of the conformational isomerization of cyclohexane by Jonas *et al.*[70] with a stochastic collisional model. Another example deals with the *cis–trans* photoisomerization of diphenylebutadiene or of the DODCI cyanine dye. Fleming and co-workers[71–74] report that their results do not agree well with the predictions of a statistical model for the activated barrier crossing in liquids proposed by Kramers.[60–61] Bagchi and Oxtoby[75] report that Fleming's results are compatible with a non-Markoffian frictional model proposed by Grote and Hynes.[62]

Stilbene results We report here on our studies[35] of the isomerization of trans-stilbene (**1**) and of a fused-ring analog trans-1,1′-biindanylidene (**2**) dissolved in linear alkanes.

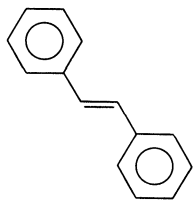

(**1**)

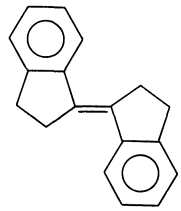

(**2**)

Since the isomerization process involves a large amplitude structural change, the rate of this reaction must depend on the friction exerted by the solvent on the solute. This study focuses therefore on the effect of the viscosity of the solvent on the isomerization rate constant. The molecules (**1**) and (**2**) have an activation energy barrier along the reaction coordinate (the torsional angle around the ethylenic double bond). It is possible that this barrier arises from an avoided crossing of a $B_u(\pi - \pi^*)$ potential surface with a surface corresponding to an A_g state. The lowest excited singlet state in the trans configuration is the B_u state, whereas the A_g state is lower in energy than the B_u

state in the twisted configuration.[76–78] The height of the barrier is estimated to be 3.5 kcal/mol for trans-stilbene and 1.5 kcal/mol for *trans*-1,1′-biindanylidene.[79]

The fluorescence lifetimes of trans-stilbene in a series of *n*-alkanes (butane-hexadecane) were measured at room temperature with an instrument consisting of a frequency-quadrupled mode-locked Nd: glass laser and a streak camera. The data could be fitted to single exponential decays. Details are given elsewhere.[35] The rate constant of the non-radiative decay process k_{nr} was calculated for each solvent according to the equation:

$$k_{nr} = \tau_F^{-1} - k_r = F(\eta)\, e^{-E_b/RT} \tag{8}$$

where τ_F is the fluorescence lifetime, k_r is the radiative rate constant, $F(\eta)$ is the viscosity-dependent frequency factor, and E_b is the height of the activation energy barrier. The non-radiative rate constants of biindanylidene were calculated from the relative fluorescence quantum yields and from the determination of the fluorescence lifetime in hexadecane. Figure 8 shows the variation of the frequency factor

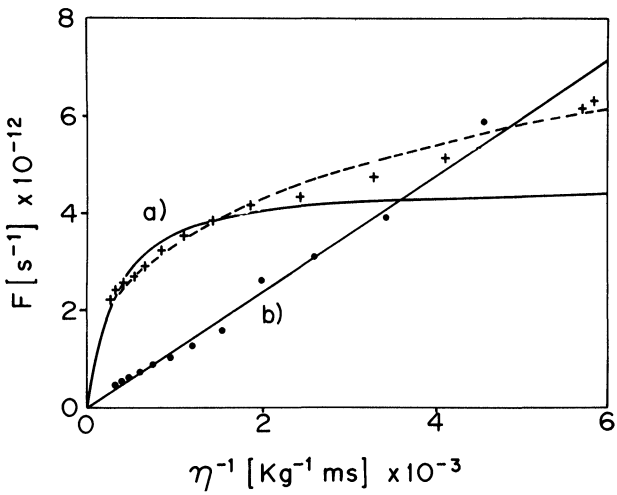

FIGURE 8 Frequency factor F from Eq. (8) as a function of the inverse of the paraffin hydrocarbon solvent shear viscosity. (a) Trans-stilbene; (b) Trans-1,1′-biindanylidene. The curves represent best fits of Kramers' model (solid lines) and Grote and Hynes'[62] model (dashed line).

F as a function of the inverse of the (shear) viscosity of the solvents for *trans*-stilbene and *trans*-biidanylidene.

The data obtained for stilbene can be compared with the model for the solvent assisted crossing over a potential barrier proposed by Kramers.[60,61] In this model, the interaction between the solvent and the solute is expressed by a random force which models the collisions of the solvent molecules and a frictional force which is proportional to the angular velocity of the moving part of the molecule. The random force averages out with time, whereas the frictional force represents the net effect of the solvent on the solute. It is supposed that the correlation function of the random force decays very rapidly in comparison with the timescale of the conformational change of the molecule. The frictional drag coefficient is then independent of time and may be calculated according to Stokes' relation. Figure 8a (solid line) depicts a fit of Kramers model to the experimental data in the region of higher viscosities. This figure shows that the fit is unsatisfactory: the curvature of the calculated curve cannot be made to agree with the experimental data.

A possible improvement is to take into account the correlations of the forces acting on the reactive motion. Such a model has been introduced by Grote and Hynes.[62] The frictional drag coefficient experienced by the moving part of the molecule is proportional to the solvent-averaged time correlation function of the forces exerted by the solvent. This time or frequency-dependent drag coefficient can be calculated from physical properties of the solvent (see Zwanzig and Bixon[80]). A fit of Grote and Hynes model to all experimental data is shown in Figure 8a (dashed line). Although the number of adjustable parameters is the same for the two models considered here, the agreement of the frequency-dependent friction model with the experimental data is much better than for the "zero-frequency component friction model" of Kramers. From this, it would seem that the isomerization rate is determined by the high frequency motion of the molecule near the top of the potential barrier. In general, this rate will depend not only on the height of the barrier but also on its shape. For sharp barriers (as seems to be the case in trans-stilbene), the residence time on top of the barrier is short. Slow motions of the alkane chains which contribute to the zero-frequency viscosity may be inefficient in promoting or preventing the barrier crossing. For high viscosities, the isomerization rate would then not be as strongly dependent on the zero-frequency viscosity as Kramers' model

predicts. This agrees with Figure 8a where the curvature predicted by Kramers' model is too large. On the other hand, the frequency-dependence of the viscosity becomes less important for flat barriers and long residence times close to the top of the barrier. In this case, Kramers' model should predict the correct viscosity dependence of the isomerization rate. In the high friction limit, this model predicts that the isomerization rate is proportional to the inverse of the viscosity. This is the viscosity dependence which has been observed for biindanylidene (see Figure 8b). A flatter barrier for biindanylidene than for trans-stilbene seems also reasonable in view of a smaller barrier height for biindanylidene.

Some questions conerning the applicability of both Kramers and Grote and Hynes models remain unanswered. Both models suppose that the isomerization process can be described by one reaction coordinate only. Comparison of the structures of stilbene and biindanylidene shows that while this unidimensionality may be correct in the case of biindanylidene the rotation of the phenyl groups around the single bond may influence the isomerization dynamics for stilbene. A second question concerns the height of the barrier. Both models considered here assume that this height is large when compared with k_BT. If this condition is fulfilled in the case of stilbene, the situation is less clear for biindanylidene. Although the concepts of frequency dependent friction and dimensionality are apparently different explanations for the comparative behavior of the two systems discussed here, they are related. The quasi-freedom of motion of the phenyl rings in stilbene must imply that the barrier crossing is stimulated by collisions that influence phenyl torsions as well as overall motion about the double bond. Thus the correlated nature of the forces would be expected to be important. In the one dimensional case delta correlated force models might be adequate.

Acknowledgements

We are deeply grateful to Professor A. B. Smith III for synthesizing the biindanylidene, and to Dr. A. G. McGhie for developing methods of purifying it.

References

1. P. M. Rentzepis, *Chem. Phys. Lett.* **2,** 117 (1968).
2. D. Huppert, J. Jortner and P. M. Rentzepis, *Isr. J. Chem.* **16,** 277 (1977).
3. R. M. Hochstrasser and R. B. Weisman, in: *Radiationless Transitions*, ed. S. H. Lin (Academic, New York, 1980).

4. R. M. Hochstrasser, H. Lutz and G. W. Scott, *Chem. Phys. Lett.* **24,** 162 (1974).
5. R. W. Anderson, R. M. Hochstrasser, H. Lutz and G. W. Scott, *Chem. Phys. Lett.* **28,** 153 (1974).
6. R. W. Anderson, R. M. Hochstrasser, H. Lutz and G. W. Scott, *J. Chem. Phys.* **61,** 2500 (1974).
7. R. W. Anderson, R. M. Hochstrasser, H. Lutz and G. W. Scott, *Chem. Phys. Lett.* **32,** 204 (1975).
8. A. Laubereau, D. von der Linde and W. Kaiser, *Phys. Rev. Lett.* **28,** 1162 (1972).
9. A. Laubereau and W. Kaiser, *Rev. Mod. Phys.* **50,** 607 (1978).
10. R. R. Alfano and S. L. Shapiro, *Phys. Rev. Lett.* **24,** 584 (1970); R. R. Alfano and S. L. Shapiro, *Chem. Phys. Lett.* **8,** 631 (1971).
11. B. I. Greene, R. M. Hochstrasser and R. B. Weisman, *J. Chem. Phys.* **70,** 1247 (1979).
12. J. P. Heritage and R. K. Jain, *Appl. Phys. Lett.* **32,** 101 (1978).
13. J. P. Heritage, in: *Picosecond Phenomena II,* ed. R. M. Hochstrasser, W. Kaiser and C. V. Shank (Springer-Verlag, Berlin, Heidelberg, New York, 1980).
14. F. Ho, W.-S. Tsay, J. Trout and R. M. Hochstrasser, *Chem. Phys. Lett.* **83,** 5 (1981).
15. K. Duppen, B. M. M. Hesp and D. A. Wiersma, *Chem. Phys. Lett.* **79,** 399 (1981).
16. C. V. Shank and E. P. Ippen, in: *Dye Lasers,* ed. F. P. Schäfer (Springer-Verlag, Berlin, Heidelberg and New York, 1977).
17. R. L. Fork, B. I. Greene and C. V. Shank, *Appl. Phys. Lett.* **38,** 671 (1981); C. V. Shank, R. L. Fork and R. T. Yen, in: *Picosecond Phenomena III,* ed. K. B. Eisenthal, R. M. Hochstrasser, W. Kaiser and A. Laubereau (Springer-Verlag, Berlin, Heidelberg and New York, 1982).
18. B. Honig, *Ann. Rev. Phys. Chem.* **29,** 31 (1978).
19. D. Holten and M. W. Windsor, *Ann. Rev. Biophys. Bioeng.* **7,** 189 (1978).
20. E. P. Ippen, C. V. Shank, A. Lewis and M. A. Marins, *Science* **200,** 1279 (1978).
21. D. Holten, C. Hoganson, M. W. Windsor, C. C. Schenck, W. W. Parson, A. Migus, R. L. Fork and C. V. Shank, *Biochim. Biophys. Acta* **592,** 461 (1980).
22. C. V. Shank, E. P. Ippen and R. Bersohn, *Science* **193,** 50 (1976).
23. B. I. Greene, R. M. Hochstrasser, R. B. Weisman and W. A. Eaton, *Proc. Natl. Acad. Sci. USA* **75,** 5255 (1978).
24. D. A. Chernoff, R. M. Hochstrasser and A. W. Steele, *Proc. Natl. Acad. Sci. USA* **77,** 5606 (1980).
25. P. A. Cornelius, R. M. Hochstrasser and A. W. Steele, *J. Mol. Biol.* in press.
26. W. G. Eisert, E. O. Degenkolb, L. J. Noe and P. M. Rentzepis, *Biophys. J.* **25,** 455 (1979).
27. K. F. Freed and A. Nitzan, *J. Chem. Phys.* **73,** 4765 (1980).
28. R. Moore, F. E. Doany, E. J. Heilweil and R. M. Hochstrasser, *Faraday Discuss. Chem. Soc.* **75,** in press.
29. S. P. Velsko and R. M. Hochstrasser, *Vibrational Dynamics in Molecular Crystals: The Separated Band Limit,* in process of publication.
30. R. Bozio, P. L. DeCola and R. M. Hochstrasser, *Vibrational Energy Decay in Solid Benzene by Coherent Raman Spectroscopy,* in process of publication.
31. F. Ho, J. Trout, W.-S. Tsay, S. P. Velsko and R. M. Hochstrasser, *Vibrational Energy Trapping in Benzene Crystals,* in process of publication.
32. I. I. Abram and R. M. Hochstrasser, *J. Chem. Phys.* **72,** 3617 (1980).
33. I. I. Abram and R. M. Hochstrasser, *J. Chem. Phys.* **75,** 337 (1981).
34. E. J. Heilweil, F. E. Doany, R. Moore and R. M. Hochstrasser, *J. Chem. Phys.* **76,** 5632 (1982).
35. G. C. Rothenberger, D. K. Negus and R. M. Hochstrasser, *Solvent Influence on Photoisomerization Dynamics,* in preparation.

36. R. M. Hochstrasser and P. Prasad, in *Excited States*, Vol. 1, ed. E. C. Lim (Academic, New York, 1974).
37. R. G. Bray and M. J. Berry, *J. Chem. Phys.* **71,** 4909 (1979).
38. J. B. Hopkins, D. E. Powers and R. E. Smalley, *J. Chem. Phys.* **72,** 5039 (1980); J. B. Hopkins, D. E. Powers, S. Mukamel and R. E. Smalley, *J. Chem. Phys.* **72,** 5049 (1980); J. B. Hopkins, D. E. Powers and R. E. Smalley, *J. Chem. Phys.* **73,** 683 (1980).
39. A. Amirav, U. Even and J. Jortner, *J. Chem. Phys.* **75,** 3770 (1981).
40. R. A. Coveleskie, D. A. Dolson and C. S. Parmenter, *J. Chem. Phys.* **72,** 5774 (1980).
41. T. M. Dunn, private communication.
42. R. A. Coveleskie and C. S. Parmenter, *J. Mol. Spectrosc.* **86,** 86 (1981).
43. S. H. Kable, W. D. Lawrence and A. E. W. Knight, *J. Phys. Chem.* **86,** 1244 (1982).
44. G. Flynn and E. Weitz, *Ann. Rev. Phys. Chem.* **25,** 275 (1974); G. Flynn, *Acc. Chem. Res.* **14,** 334 (1981).
45. G. Renner and M. Maier, *Chem. Phys. Lett.* **28,** 614 (1974); G. Ewing, *Chem. Phys. Lett.* **30,** 485 (1975).
46. S. R. J. Bueck and R. M. Osgood, *Chem. Phys. Lett.* **39,** 568 (1976).
47. E. W. Knapp and S. F. Fischer, *Chem. Phys.* **63,** 203 (1981).
48. A. Fendt, S. F. Fischer and W. Kaiser, *Chem. Phys.* **57,** 55 (1981); *Chem. Phys. Lett.* **82,** 350 (1981).
49. A. Laubereau, S. F. Fischer, K. Spanner and W. Kaiser, *Chem. Phys.* **31,** 335 (1978).
50. R. Kubo, in: Fluctuations, Relaxation, and Resonance in Magnetic Systems, ed. D. ter Haar (Plenum Press, New York, 1962).
51. S. F. Fischer and A. Laubereau, *Chem. Phys. Lett.* **35,** 6 (1975).
52. T. Kato and T. Tanaka, *Chem. Phys. Lett.* **62,** 77 (1979).
53. F. G. Baglin and L. M. Wilkes, *J. Phys. Chem.* **85,** 3643 (1981).
54. R. L. Frost, D. W. James, R. Appleby and R. E. Mayes, *J. Phys. Chem.* **86,** 3840 (1982).
55. J. Lascombe and M. Perrot, *J. Chem. Soc. Farad. Disc.* **66,** 216 (1978).
56. S. A. Rice and M. G. Sceats, *J. Phys. Chem.* **85,** 1108 (1981); Y. Katoaka, H. Hamada, S. Nose and T. Yamamoto, *J. Chem. Phys.* **77,** 5699 (1982).
57. D. B. McDonald, J. Rossel and G. R. Fleming, *IEEE J. Quant. Elec.* **QE17,** 1134 (1981).
58. J. Califano and co-workers, private communication.
59. S. A. Adelman, Chemical reaction dynamics in liquid solution, in: *Adv. Phys. Chem.*, in press.
60. H. A. Kramers, *Physica* **VII,** 284 (1940).
61. S. Chandrasekhar, *Rev. Mod. Phys.* **15,** 1 (1943).
62. F. R. Grote and J. T. Hynes, *J. Chem. Phys.* **73,** 2715 (1980).
63. K. Schulten, Z. Schulten and A. Szabo, *J. Chem. Phys.* **74,** 4426 (1981).
64. J. Skolnick and E. Helfand, *J. Chem. Phys.* **72,** 5489 (1980).
65. J. L. Skinner and P. G. Wolynes, *J. Chem. Phys.* **69,** 2143 (1978).
66. J. L. Skinner and P. G. Wolynes, *J. Chem. Phys.* **72,** 4913 (1980).
67. J. A. Montgomery, D. Chandler and B. J. Berne, *J. Chem. Phys.* **70,** 4056 (1979).
68. J. A. Montgomery, S. L. Holmgren and D. Chandler, *J. Chem. Phys.* **73,** 3688 (1980).
69. D. K. Garrity and J. L. Skinner, *Chem. Phys. Lett.* **95,** 46 (1983).
70. D. L. Hasha, T. Eguchi and J. Jonas, *J. Chem. Phys.* **75,** 1571 (1981).
71. S. P. Velsko and G. R. Fleming, *Chem. Phys.* **65,** 59 (1982).
72. S. P. Velsko and G. R. Fleming, *J. Chem. Phys.* **76,** 3553 (1982).

73. S. P. Velsko, D. H. Waldeck and G. R. Fleming, *J. Chem. Phys.* **78,** 249 (1983).
74. K. E. Kerry and G. R. Fleming, *Chem. Phys. Lett.* **93,** 322 (1982).
75. B. Bagchi and D. W. Oxtoby, *J. Chem. Phys.* **78,** 2735 (1983).
76. G. Orlandi and W. Siebrand, *Chem. Phys. Lett.* **30,** 352 (1975).
77. P. Tavan and K. Schulten, *Chem. Phys. Lett.* **56,** 200 (1978).
78. G. Orlandi, P. Palmieri and G. Poggi, *J. Am. Chem. Soc.* **101,** 3492 (1979).
79. J. Saltiel and J. T. d'Agostino, *J. Am. Chem. Soc.* **94,** 6445 (1972).
80. R. Zwanzig and M. Bixon, *Phys. Rev. A* **2,** 2005 (1970).